

# Radiative Decay Width Measurements of Neutral Kaon Excitations Using the Primakoff Effect

A. Alavi-Harati<sup>12</sup>, T. Alexopoulos<sup>12</sup>, M. Arenton<sup>11</sup>, K. Arisaka<sup>2</sup>, S. Averitte<sup>10</sup>,  
R.F. Barbosa<sup>7,\*\*</sup>, A.R. Barker<sup>5</sup>, M. Barrio<sup>4</sup>, L. Bellantoni<sup>7</sup>, A. Bellavance<sup>9</sup>, J. Belz<sup>10</sup>,  
D.R. Bergman<sup>10</sup>, E. Blucher<sup>4</sup>, G.J. Bock<sup>7</sup>, C. Bown<sup>4</sup>, S. Bright<sup>4</sup>, E. Cheu<sup>1</sup>, S. Childress<sup>7</sup>,  
R. Coleman<sup>7</sup>, M.D. Corcoran<sup>9</sup>, G. Corti<sup>11</sup>, B. Cox<sup>11</sup>, A. Cunha<sup>10</sup>, A.R. Erwin<sup>12</sup>, R. Ford<sup>7</sup>,  
A. Glazov<sup>4</sup>, A. Golossanov<sup>11</sup>, G. Graham<sup>4</sup>, J. Graham<sup>4</sup>, E. Halkiadakis<sup>10</sup>, J. Hamm<sup>1</sup>,  
K. Hanagaki<sup>8</sup>, S. Hidaka<sup>8</sup>, Y.B. Hsiung<sup>7</sup>, V. Jejer<sup>11</sup>, D.A. Jensen<sup>7</sup>, R. Kessler<sup>4</sup>,  
H.G.E. Kobrak<sup>3</sup>, J. LaDue<sup>5</sup>, A. Lath<sup>10</sup>, A. Ledovskoy<sup>11</sup>, P.L. McBride<sup>7</sup>, D. Medvigy<sup>10</sup>,  
P. Mikelsons<sup>5</sup>, E. Monnier<sup>4,\*</sup>, T. Nakaya<sup>7</sup>, K.S. Nelson<sup>11</sup>, H. Nguyen<sup>7</sup>, V. O'Dell<sup>7</sup>,  
R. Pordes<sup>7</sup>, V. Prasad<sup>4</sup>, X.R. Qi<sup>7</sup>, B. Quinn<sup>4</sup>, E.J. Ramberg<sup>7</sup>, R.E. Ray<sup>7</sup>, A. Roodman<sup>4</sup>,  
S. Schnetzer<sup>10</sup>, K. Senyo<sup>8</sup>, P. Shanahan<sup>7</sup>, P.S. Shawhan<sup>4</sup>, J. Shields<sup>11</sup>, W. Slater<sup>2</sup>,  
N. Solomey<sup>4</sup>, S.V. Somalwar<sup>10,†</sup>, R.L. Stone<sup>10</sup>, E.C. Swallow<sup>4,6</sup>, S.A. Taegar<sup>1</sup>,  
R.J. Tesarek<sup>10</sup>, G.B. Thomson<sup>10</sup>, P.A. Toale<sup>5</sup>, A. Tripathi<sup>2</sup>, R. Tschirhart<sup>7</sup>, S.E. Turner<sup>2</sup>,  
Y.W. Wah<sup>4</sup>, J. Wang<sup>1</sup>, H.B. White<sup>7</sup>, J. Whitmore<sup>7</sup>, B. Winstein<sup>4</sup>, R. Winston<sup>4</sup>,  
T. Yamanaka<sup>8</sup>, E.D. Zimmerman<sup>4</sup>

<sup>1</sup> University of Arizona, Tucson, Arizona 85721

<sup>2</sup> University of California at Los Angeles, Los Angeles, California 90095

<sup>3</sup> University of California at San Diego, La Jolla, California 92093

<sup>4</sup> The Enrico Fermi Institute, The University of Chicago, Chicago, Illinois 60637

<sup>5</sup> University of Colorado, Boulder, Colorado 80309

<sup>6</sup> Elmhurst College, Elmhurst, Illinois 60126

<sup>7</sup> Fermi National Accelerator Laboratory, Batavia, Illinois 60510

<sup>8</sup> Osaka University, Toyonaka, Osaka 560-0043 Japan

<sup>9</sup> Rice University, Houston, Texas 77005

<sup>10</sup> Rutgers University, Piscataway, New Jersey 08854

<sup>11</sup> The Department of Physics and Institute of Nuclear and Particle Physics, University of Virginia,  
Charlottesville, Virginia 22901

<sup>12</sup> University of Wisconsin, Madison, Wisconsin 53706

\* Permanent address C.P.P. Marseille/C.N.R.S., France

\*\*Permanent address University of São Paulo, São Paulo, Brazil

† To whom correspondence should be addressed. Electronic address: somalwar@physics.rutgers.edu

**The KTeV Collaboration**

## Abstract

We produce a sample consisting of 147 candidate events, with minimal backgrounds, of the mixed axial vector pair ( $K_1(1270)$ - $K_1(1400)$ ) by exciting  $K_L$ 's in the Coulomb field of lead and report the first measurements of the radiative widths  $\Gamma_r(K_1(1400)) = 280.8 \pm 23.2(stat) \pm 40.4(syst)$  keV and  $\Gamma_r(K_1(1270)) = 73.2 \pm 6.1(stat) \pm 28.3(syst)$  keV. We also place 90% CL upper limits  $\Gamma_r(K^*(1410)) \leq 52.9$  keV for the vector state and  $\Gamma_r(K_2^*(1430)) \leq 5.4$  keV for the tensor state. These measurements allow for significant tests of quark-model predictions of radiative widths for the low-lying vector mesons.

Several resonant excitations of the neutral kaon are known to exist [1], most having been observed *indirectly* using partial wave analysis [2]. Figure 1 is a schematic representation of the neutral kaon excitations with central masses less than  $1.5 \text{ GeV}/c^2$ . The axial vector pair ( $K_1(1270)$ - $K_1(1400)$ ) is interesting because it is a (coherent) mixture of the singlet  $^1P_1$  and the triplet  $^3P_1$  states [3], parameterized by the mixing angle  $\Theta$ :  $K_1(1270) = -^3P_1 \cdot \sin \Theta + ^1P_1 \cdot \cos \Theta$  and  $K_1(1400) = ^3P_1 \cdot \cos \Theta + ^1P_1 \cdot \sin \Theta$ . The radiative decay widths of the kaon excitations,  $\Gamma_r(K^*) = \Gamma(K^* \rightarrow K + \gamma)$ , are sensitive to the magnetic moments of the constituent quarks [4]. Radiative widths have been calculated for low-lying mesons using both a dynamic quark model [5] and a relativistic quark model [6,7]. Experimentally, only  $\Gamma_r(K^*(892))$  has been measured [8] so far.

The Primakoff effect [9], i.e. excitation by the Coulomb field, can be used to measure radiative widths since it is the inverse of radiative decay. In this Letter, we use the full dataset collected during the 1996-97 run of the KTeV experiment at Fermilab to study Primakoff production in two channels: the six-body  $K^*(892)\pi^0$  channel, exemplified by  $K^*(1410)$  or  $K_1(1400) \rightarrow K^*(892)\pi^0 \rightarrow [K_S\pi^0]\pi^0 \rightarrow [(\pi^+\pi^-)(\gamma\gamma)](\gamma\gamma)$ , which has two  $\pi^0$ 's, and the four-body  $K_S\pi^0$  channel, exemplified by  $K^*(892)$  or  $K^*(1410) \rightarrow K_S\pi^0 \rightarrow (\pi^+\pi^-)(\gamma\gamma)$ , which has a single  $\pi^0$ . In the  $K^*(892)\pi^0$  channel, we observe 147 candidate events which are predominantly the axial vector  $K_1(1400)$  with a small admixture of  $K_1(1270)$ . Using a large sample of  $K^*(892)$ 's from the  $K_S\pi^0$  channel for normalization, we report the first measurements of the radiative widths for the axial vector pair. We also use the  $K_S\pi^0$  channel to place the first upper limit on  $\Gamma_r(K^*(1410))$  and a stringent upper limit on  $\Gamma_r(K_2^*(1430))$ .

For high particle energies and small production angles, the rate of exciting a  $K_L$  to a  $K^*$  in the Coulomb field of a nucleus A is given by [10]

$$\frac{d\sigma}{dt}(K_L + A \rightarrow K^* + A) = \pi\alpha Z^2 \left( \frac{2S_{K^*} + 1}{2S_K + 1} \right) \frac{\Gamma(K^* \rightarrow K + \gamma)}{k^3} \frac{t'}{t^2} |f_{EM}|^2, \quad (1)$$

where  $\alpha$  is the fine structure constant,  $Z$  is the atomic number of the nucleus,  $S_K$  and  $S_{K^*}$  are the spins of  $K_L$  and the resonance, respectively,  $k = (m_{K^*}^2 - m_K^2)/2m_{K^*}$ ,  $t$  is the magnitude of the square of the momentum transfer and  $t' = t - t_{min}$ ,  $\sqrt{t_{min}} = (m_{K^*}^2 - m_K^2)/2P_K$ , where  $P_K$  is the laboratory momentum of the  $K_L$ . Finally,  $f_{EM}$  is the nuclear electric form factor. Thus, the rate of Primakoff production is directly proportional to the radiative width.

KTeV utilized an 800 GeV/c proton beam to generate two neutral beams consisting kaons, neutrons and some hyperons. In the E832 configuration [11], one of the beams

passed through a regenerator which was located  $\sim 124$  m from the target. The regenerator consisted of 84 modules of 2cm-thick plastic scintillator followed by a module composed of a lead-scintillator sandwich. Since the Primakoff effect is proportional to  $Z^2$  of the target material, more than 98% of the observed Primakoff excitations (equation 1) were produced in the final lead pieces. The regenerator was instrumented with photomultiplier tubes which enabled us to tag and reject backgrounds from inelastic interactions. We detect  $\pi^+\pi^-$  tracks from  $K_S$  decays using a drift chamber spectrometer system and photons from  $\pi^0$  decays using a pure CsI electromagnetic calorimeter. The event trigger was initiated by signals from two scintillator hodoscopes located downstream of the spectrometer and required hits in the drift chambers consistent with two oppositely charged tracks. The decay volume was surrounded by a near-hermetic set of devices to veto photons.

In the offline analysis, the fiducial region for the decay vertex of  $K_S \rightarrow \pi^+\pi^-$  is restricted to 15 m downstream of the regenerator. We reconstruct  $\pi^0$ 's using pairs of energy clusters in the calorimeter. The clusters are required to have energies greater than 1 GeV and photon-like spatial distributions. To reject electrons, we require that the ratio of energy deposited in the calorimeter to the particle momentum as measured by the spectrometer be  $< 0.8$ .

To reconstruct the  $K^*(892) \rightarrow K_S\pi^0$  decays used for normalization, in the four-body channel we require the invariant masses of the  $\gamma\gamma$  and the  $\pi^+\pi^-$  to be within 10 MeV/c<sup>2</sup> of the  $\pi^0$  and  $K_S$  invariant masses, respectively. We isolate Primakoff (forward) production by demanding that the square of the transverse momentum ( $p_t^2$ ) of the  $\pi^+\pi^-\gamma\gamma$  with respect to a line connecting the target and the decay vertex of  $K^*(892)$  be less than 0.001 (GeV/c)<sup>2</sup>. We further require  $\pi^+\pi^- p_t^2 > 0.01$  (GeV/c)<sup>2</sup> because the *daughter*  $K_S$  recoils against the  $\pi^0$ . The resulting sample of 29,399  $K^*(892) \rightarrow K_S\pi^0$  decays with  $K_S$  energy between 30 and 210 GeV, and the  $K^*(892)$  energy between 55 and 225 GeV is shown in figure 2(top).

The requirements for the  $K^*(892)\pi^0$  six-body channel are similar, except for changes to account for the extra  $\pi^0$  and differences in kinematics. The photon pairings for the two  $\pi^0$ 's are determined using a  $\chi^2$  formed by comparing  $M_{\gamma\gamma}$  and  $M_{\pi^+\pi^-\gamma\gamma}$  to the known masses of  $\pi^0$  and  $K^*(892)$ , respectively. The  $K_S\pi^0$  mass for the *daughter*  $K^*(892)$  is required to be within 101 MeV/c<sup>2</sup> (two mass-widths) of the  $K^*(892)$  mass and its  $p_t^2$  to be  $> 0.03$  (GeV/c)<sup>2</sup>. The  $p_t^2$  cut also serves to eliminate background from Primakoff-produced  $K^*(892)$ 's when accompanied by an accidental  $\pi^0$ . To eliminate events in which two kaons decay to a charged and a neutral pion pair, we remove events for which the four-photon invariant mass is within 20 MeV of the  $K_L$  mass. The resulting sample of  $(K_S\pi^0)\pi^0$  events with total energy greater than 90 GeV is depicted in figure 3 and shows a clustering near 1.4 GeV/c<sup>2</sup>. The mass projection shows the resonant signature exhibited by events with  $p_t^2 < 0.001$  (GeV/c)<sup>2</sup> and the  $p_t^2$  projection shows the sharp fall-off confirming Primakoff production. There are 147 events within the mass fiducial region (1.1-1.64 GeV/c<sup>2</sup>). Figure 4 shows the invariant mass and  $p_t^2$  of the daughter  $K^*(892)$  where the  $p_t^2$  displays a Jacobian distribution expected of a daughter particle in a two-body decay.

The possible candidates for the observed  $K^*(892)\pi^0$  resonance are  $K_0^*(1430)$ , K(1460),  $K^*(1410)$ ,  $K_2^*(1430)$ ,  $K_1(1270)$ , and  $K_1(1400)$  (figure 1). The selectivity of the Primakoff effect rules out  $K_0^*(1430)$  and K(1460) because of spin-parity conservation and the  $J=0 \not\leftrightarrow J=0$  selection rule, respectively. Contributions from the vector  $K^*(1410)$  and tensor  $K_2^*(1430)$  can be eliminated because both have significant branching fractions to  $K_S\pi^0$  [1], yet we see no evidence for their presence in this  $(K_S\pi^0)$  channel; note the lack of resonance near 1.4 GeV/c<sup>2</sup>

in figure 2 (bottom). We fit a combination of  $K^*(892)$  and  $K^*(1410)(K_2^*(1430))$  simulations to the data and confirm that the signal from  $K^*(1410)(K_2^*(1430))$  in the  $K_S\pi^0$  channel is consistent with zero:  $4.0 \pm 6.0(0.1 \pm 3.8)$   $K^*(1410)(K_2^*(1430))$  events. Using the known branching fractions [1] of  $K^*(1410)$  and  $K_2^*(1430)$  to  $K_S\pi^0$  and  $K^*(892)\pi^0$ , we translate these results into a negligible  $2.4 \pm 3.6(0.0 \pm 0.7)$  event contribution of  $K^*(1410)(K_2^*(1430))$  in the  $K^*(892)\pi^0$  channel. Thus we are left with only the axial vector pair ( $K_1(1270)$ - $K_1(1400)$ ) as a possible candidate for the observed resonance in the  $K^*(892)\pi^0$  channel.

We cross-checked the axial vector nature of the observed signal using the distributions of Gottfried-Jackson (GJ) angles  $\dagger$   $\theta$  and  $\phi$ . These distributions generally confirm our axial vector assignment. However, due to the relatively strong angular dependence of the detector acceptance, they do not have strong discrimination power between the axial vector pair and  $K^*(1410)$  and  $K_2^*(1430)$ .

We now compute the radiative widths for the axial vector pair. It is difficult to decompose the mass spectrum of the observed signal into  $K_1(1270)$  and  $K_1(1400)$  because their mass separation is comparable to their widths. Nonetheless, mass information alone tells us that the contribution from  $K_1(1270)$  is slight: only  $8.8 \pm 8.6$  events are due to  $K_1(1270)$ . However, a significantly better resolution is possible because the Primakoff effect can produce only the singlet ( $^1P_1$ ) component of the axial vector pair [13] and the singlet-triplet mixing angle  $\Theta$  has been measured. Using  $\Theta = 56 \pm 3^\circ$  [2] together with the known branching ratios of  $K_1(1270)$  and  $K_1(1400)$ , we resolve the observed signal into  $11.4 \pm 1.0(stat) \pm 4.1(ext\ syst)$   $K_1(1270)$  events and  $134.4 \pm 11.1(stat) \mp 4.1(ext\ syst)$   $K_1(1400)$  events, where the (external) systematic error is due to the measurement uncertainties in the mixing parameter  $\Theta$  and in the  $K_1(1270)$  and  $K_1(1400)$  branching fractions to the  $K^*(892)\pi^0$  channel. This decomposition, depicted in figure 3, leads to  $\Gamma_r(K_1(1270)) = 73.2 \pm 6.1(stat) \pm 8.2(int\ syst) \pm 27.0(ext\ syst)$  keV and  $\Gamma_r(K_1(1400)) = 280.8 \pm 23.2(stat) \pm 31.4(int\ syst) \pm 25.4(ext\ syst)$  keV, where we have used our  $K^*(892)$  sample (figure 2) for normalization purposes since  $\Gamma_r(K^*(892))$  is known experimentally [8]. Our measurements share internal systematic errors of 8.7% due to uncertainties in the strong production (discussed below), 6.6% due to detector acceptance effects, and 2.4% due to the 3.6 event uncertainty in the possible contributions from  $K^*(1410)$  and  $K_2^*(1430)$ , as discussed earlier. The uncertainty in the  $K^*(892)$  radiative width measurement [8] causes an additional 8.5% (external) systematic error.

Primakoff production is characterized by a sharp ( $\sim t^{-1}$ ) forward production (equation 1) allowing a strict  $p_t^2 < 0.001(GeV/c)^2$  cut which virtually eliminates all potential backgrounds; see figure 3. Based on an extrapolation from the large  $p_t^2 (> 0.1 (GeV/c)^2)$  region, we estimate 1.2 events out of 147 signal candidate events to be due to incoherent production and other possible backgrounds such as those from the decay products of the  $\Lambda$ 's and  $\phi$ 's produced when neutrons in the beam interact with the regenerator.

Coherent strong production and its interference (with unknown strength) with Primakoff production are expected to be small at our energies [8]. Indeed, a maximum likelihood fit in the  $p_t^2$  variable for the strong production and the strength of the strong-Coulomb interference using the prescription given in [8,14] indicates that the strength of interference preferred by

---

$\dagger$ In the GJ frame the excited kaon is at rest at the origin, the z-axis is along the momentum of the incoming  $K_L$  and the y-axis is perpendicular to the production plane [12].

our data is consistent with zero. A constructive (destructive) interference would mean that the actual number of Primakoff events is less (more) than what we observe. The mean change in our estimate of Primakoff production corresponding to one standard deviation variation in the interference strength is 8.7%, which we have taken to be the systematic error due to the uncertainties in strong production.

Earlier, we used the absence of a resonance in the  $K_S\pi^0$  channel at  $\sim 1.4$  GeV/ $c^2$  (figure 2) to limit the  $K^*(1410)$  and  $K_2^*(1430)$  contributions to the observed ( $K_1(1270)$ - $K_1(1400)$ ) axial vector pair signal. A further benefit of this finding is that we are able to limit the radiative widths  $\Gamma_r(K^*(1410))$  and  $\Gamma_r(K_2^*(1430))$  to 52.9 and 5.4 keV, respectively, at 90% CL.  $\Gamma_r(K^*(1410))$  has not been examined experimentally before, whereas  $\Gamma_r(K_2^*(1430))$  was previously limited to 84 keV at 90% CL [8]. The  $\Gamma_r(K_2^*(1430))$  limit is far stricter than the  $\Gamma_r(K^*(1410))$  limit principally because the branching fraction for  $K_2^*(1430) \rightarrow K_S\pi^0$  is substantially larger [1] than the same for  $K^*(1410) \rightarrow K_S\pi^0$ .

The predicted radiative widths for the axial vector mesons [15], are 538 keV for  $K_1(1400)$  and 175 keV for  $K_1(1270)$ ; compare to our results,  $280.8 \pm 46.6$  keV and  $73.2 \pm 28.9$  keV, respectively. We note that the theoretical model in [15] is very sensitive to the quark masses ( $m_{u,s}$ ) and rms momenta ( $\beta_{uu,us,ss}$ ) of the quarks within the mesons. The predictions are based on certain choices for  $m$  and  $\beta$ , but other choices with up to 30% variation in  $m$  are possible.

Our 90% CL upper limit on the vector  $K^*(1410)$  radiative width is 52.9 keV. In the naive quark model, this state is the first radial excitation of  $K^*(892)$  and its radiative width calculation should be similar to that for  $K^*(892)$ , for which  $\Gamma_r(K^*(892)) = 116.5 \pm 9.9$  keV [8]. The smaller value for  $K^*(1410)$  may be due to a reduced overlap of the quark wavefunction for this higher radial excitation, but further guidance from theory is needed.

Finally, we have substantially improved the upper limit on the radiative width of the tensor  $K_2^*(1430)$  from 84 keV [8] to 5.4 keV (at 90% CL). Babcock and Rosner [13] used  $SU(3)$  invariance to predict that excitations with  $J^{PC} = 1^{++}$  or  $2^{++}$  would have vanishing radiative widths. In the limit of  $SU(3)$ ,  $K_2^*(1430)$  has  $C = +1$ ; thus, our limit lends support to Babcock and Rosner's prediction [13] and serves as a direct test of the naive quark model and  $SU(3)$ -breaking.

We thank J. Bronzan for theoretical guidance and gratefully acknowledge the support and effort of the Fermilab staff and the technical staffs of the participating institutions for their vital contributions. This work was supported in part by the U.S. Department of Energy, The National Science Foundation and The Ministry of Education and Science of Japan. In addition, A.R.B., E.B. and S.V.S. acknowledge support from the NYI program of the NSF; A.R.B. and E.B. from the Alfred P. Sloan Foundation; E.B. from the OJI program of the DOE; K.H., T.N. and M.S. from the Japan Society for the Promotion of Science; and R.F.B. from the Fundação de Amparo à Pesquisa do Estado de São Paulo. P.S.S. acknowledges receipt of a Grainger Fellowship.

FIGURES

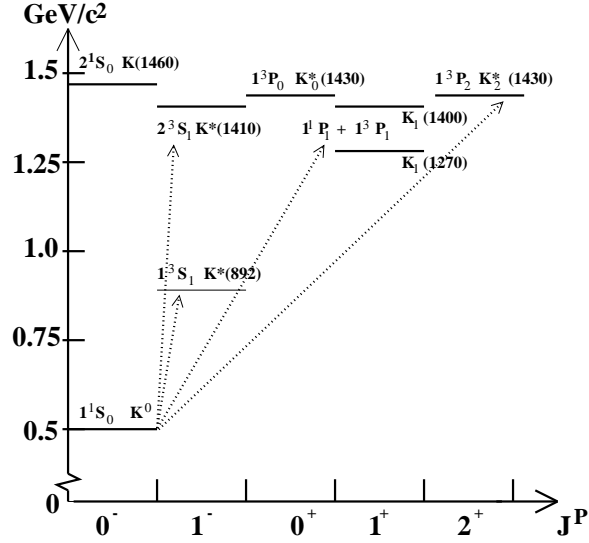


FIG. 1. Mass vs. angular momentum and parity ( $J^P$ ) for neutral kaon resonances. Arrows indicate resonances accessible by Primakoff excitation.

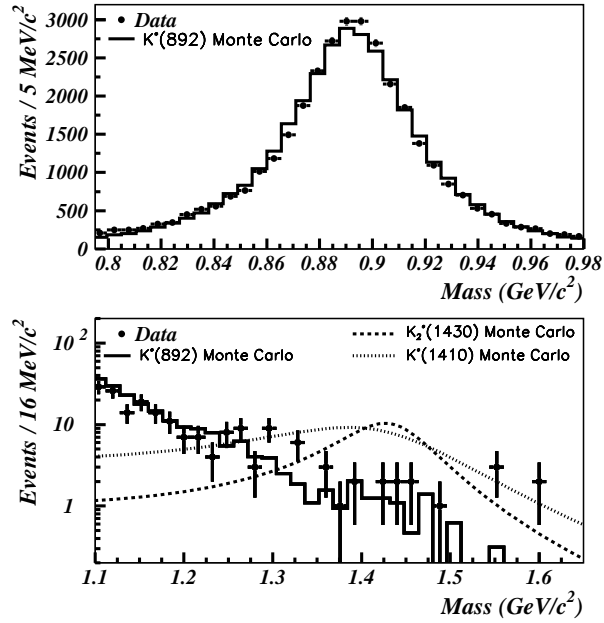


FIG. 2. Top:  $K_S\pi^0$  invariant mass in the four-body channel showing  $K^*(892) \rightarrow K_S\pi^0$  decays. Bottom: The same  $K_S\pi^0$  invariant mass in the 1.4  $\text{GeV}/c^2$  region.  $K_2^*(1430)$  and  $K^*(1410)$  simulations are also shown to arbitrary scale. No  $K_2^*(1430)$  or  $K^*(1410)$  resonance is apparent.

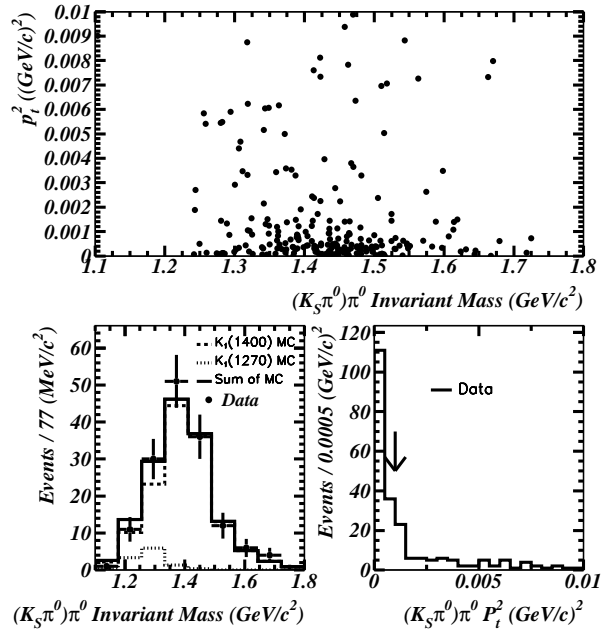


FIG. 3. Top:  $(K^*(892)\pi^0) p_t^2$  vs. invariant mass after all other cuts. Bottom Left: Projection onto the abscissa after the  $p_t^2$  cut. Decomposition of the observed signal into  $K_1(1270)$  and  $K_1(1400)$  is also shown. Bottom Right: Projection onto the ordinate after the mass cut. Note the sharply forward nature of Primakoff production.

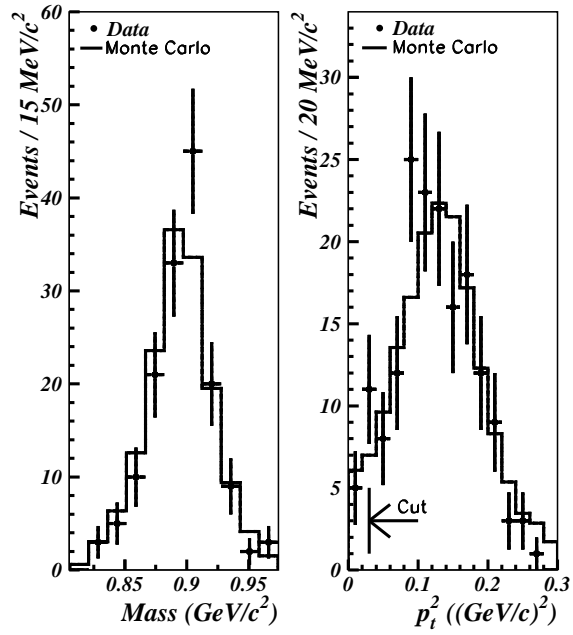


FIG. 4. Data/MC comparisons for the  $K_S\pi^0$  invariant mass (left) and the  $p_t^2$  for the observed  $(K_1(1270)-K_1(1400)) \rightarrow K^*(892)\pi^0$  signal (right). A Jacobian distribution in  $p_t^2$  indicates the recoil of the daughter  $K^*(892)$  against the  $\pi^0$ . We discard events to the left of the arrow.

## REFERENCES

- [1] R. M. Barnett et al., Phys. Rev. D54, 1 (1996).
- [2] C. Daum et al., Nuc Phys B187 (1981) 1.
- [3] M.G. Bowler et al., Nucl. Phys. B74 (1974) 493.
- [4] C. Becchi and G. Morpurgo, Phys. Rev. 140, B687 (1965).
- [5] N. Barik and P. C. Dash, Phys. Rev. D49, 299 (1993).
- [6] R. K. Das, A. R. Panda, and R. K. Sahoo, Int. J. Mod. Phys., A14, 1759 (1998).
- [7] N. Godfrey and N. Isgur, Phys. Rev. D32, 189 (1985).
- [8] D. Carlsmith, Ph.D. thesis, University of Chicago, 1984 (unpublished); D. Carlsmith *et al*, Phys. Rev. Lett. 56, 18 (1986).
- [9] H. Primakoff, Phys. Rev. Lett. 81, 899 (1951); A. Halperin, C. M. Anderson, and H. Primakoff, Phys. Rev. Lett. 152, 1295 (1966).
- [10] G. Berlاد et al., Annals of Physics 75, 461 (1973).
- [11] A. Alavi-Harati et al., Phys. Rev. Lett. 83 (1999) 22.
- [12] K. Gotfried and J. D. Jackson, Nuovo Cimento 34 1655 (1964).
- [13] J. Babcock and J. L. Rosner, Phys. Rev. D 14, 1286 (1976).
- [14] G. Faldt et al., Nucl. Phys. B41, 125 (1972); G. Faldt, Nucl. Phys. B43 591 (1972); C. Bemporad et al., Nucl. Phys. B51, 1 (1973).
- [15] I. G. Aznauryan and K. A. Oganessian Sov. J. Nucl. Phys. 47 (6), 1097 (1988).